

Uncertainty-Aware Lidar Place Recognition in Novel Environments

Keita Mason^{1,2}, Joshua Knights^{1,2}, Milad Ramezani¹, Peyman Moghadam^{1,2}, Dimity Miller²

Abstract—State-of-the-art approaches to lidar place recognition degrade significantly when tested on novel environments that are not present in their training dataset. To improve their reliability, we propose uncertainty-aware lidar place recognition, where each predicted place match must have an associated uncertainty that can be used to identify and reject potentially incorrect matches. We introduce a novel evaluation protocol designed to benchmark uncertainty-aware lidar place recognition, and present Deep Ensembles as the first uncertainty-aware approach for this task. Testing across three large-scale datasets and three state-of-the-art architectures, we show that Deep Ensembles consistently improves the performance of lidar place recognition in novel environments. Compared to a standard network, our results show that Deep Ensembles improves the Recall@1 by more than 5% and AuPR by more than 3% on average when tested on previously unseen environments. Our code repository will be made publicly available upon acceptance at <https://github.com/csiro-robotics/Uncertainty-LPR>.

I. INTRODUCTION

Localisation is a crucial capability of mobile robots – with an understanding of its location in a map, a robot can navigate to new locations, monitor an environment, and collaborate with other entities. Lidar Place Recognition (LPR) algorithms use point clouds to enable robot localisation – a robot can compare a recently captured point cloud with a map of previous point clouds to identify its current location, where the map can be generated on-the-fly or offline. These recognised locations, *i.e.*, revisit areas, can be used as loop closure constraints in a Simultaneous Localisation and Mapping (SLAM) algorithm to mitigate drift, or provide re-localisation in GPS-denied environments.

Recent research has focused on deep learning techniques for LPR [1]–[6]. During training, deep networks learn to reduce point clouds to “descriptors” that encode structural features from the environment, where similar locations have similar descriptors, and dissimilar locations have dissimilar descriptors. State-of-the-art LPR methods exhibit impressive localisation performance when tested on environments included in the training dataset [4]–[6]. However, when tested on a *novel environment*, *i.e.*, an environment not in the training dataset, their performance drops substantially.

We show an example of this in Fig. 1 – MinkLoc3D [4] achieves 93% recall when trained and tested on urban road scenes from the U.K., but this drops to 61% when tested on urban road scenes from South Korea. This performance

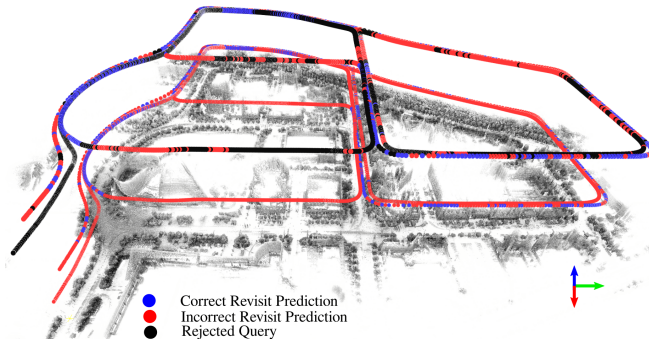


Fig. 1: The bottom traversal shows the performance of MinkLoc3D [4] when trained on Oxford road scenes, but tested on road scenes from the Daejeon Convention Centre in South Korea. Tested on this novel environment, MinkLoc3D predicts many false revisits. In the top traversal, we show our proposed approach to uncertainty-aware LPR, where uncertainty is used to reject the 50% most uncertain queries – eliminating many false revisit predictions and retaining the correct revisit predictions.

degradation highlights a critical weakness of state-of-the-art LPR techniques – an inability to generalise to conditions not represented in the training dataset. This raises questions about the true utility and reliability of existing approaches for robotics applications, which may require a robot to navigate between multiple complex and evolving environments.

Uncertainty-aware deep networks are an established approach for enabling reliable performance in novel conditions [7], [8]. Alongside each prediction, a network provides an estimate of its uncertainty, where high uncertainty indicates the network does not know and is likely to make a mistake. While uncertainty-aware deep networks have been widely explored in many computer vision fields [9]–[12], no existing research explores uncertainty estimation for LPR.

To address this, we investigate the task of *uncertainty-aware Lidar Place Recognition*. The contributions of this work are as follows:

- We present the first approach to uncertainty-aware LPR, using Deep Ensembles of state-of-the-art LPR networks. Our approach utilises uncertainty to identify and reject incorrect revisit predictions, while retaining correct revisit predictions (see Fig. 1).
- We introduce a new evaluation protocol to benchmark uncertainty-aware LPR, with dataset splits that specifically test performance in novel environments and metrics that quantify both place recognition and uncertainty estimation performance.
- We implement state-of-the-art techniques for uncertainty-aware image retrieval, and show these image-based techniques do not transfer to LPR.

¹Authors are with the Robotics and Autonomous Systems, DATA61, CSIRO, Brisbane, QLD 4069, Australia. ²Authors are with the Queensland University of Technology (QUT), Brisbane, Australia.

D.M. acknowledges ongoing support from the QUT Centre for Robotics. Author contact emails: {keita.graves, joshua.knights, milad.ramezani, peyman.moghadam}@data61.csiro.au, d24.miller@qut.edu.au

II. RELATED WORK

We first review the state-of-the-art LPR algorithms, and then discuss existing research into uncertainty estimation in retrieval tasks.

A. Lidar Place Recognition

Lidar Place Recognition (LPR) utilising 3D point clouds has been significantly explored in the last few years. LPR approaches identify similar places (revisited areas) by encoding high-dimensional point clouds into discriminative embeddings (often referred to as descriptors). Handcrafted LPR methods [13]–[17] generate local descriptors by segmenting point clouds into patches, or global descriptors that show the relationship between all the points in a point cloud.

Recent state-of-the-art LPR approaches have been dominated by deep learning-based architectures due to their impressive performance. These approaches typically utilise a backbone architecture to extract local features from the point cloud, which are then aggregated into a global descriptor.

The specific design of these components varies significantly between different works; PointNet [18], graph neural networks [3], transformers [2], [6], [19], and sparse-voxel convolutional networks [4]–[6], [20] have all been proposed as local feature extractors, and aggregation methods include NetVLAD [21], Generalised Mean Pooling (GeM) [22] and second-order pooling [5], [23]. In our evaluation, we test with networks featuring varied architecture designs: PointNetVLAD [18], MinkLoc3D [4], and TransLoc3D [6].

B. Uncertainty Estimation for Retrieval Tasks

Though there are many works exploring uncertainty estimation in lidar object detection [24]–[28] and point cloud segmentation [29], no existing works explore uncertainty estimation for LPR. While recent work by Knights *et al.* [30] shares a similar motivation to our work – reliable performance in novel environments – they explore incremental learning and specifically the issue of catastrophic forgetting.

Image retrieval is a field of computer vision that shares a similar problem setup to LPR (though notably operating on images rather than point clouds). When estimating uncertainty for image retrieval, recent works learn an uncertainty estimate by adding additional heads to their network architecture [31]–[33]. Shi *et al.* [31] examine uncertainty-aware facial recognition, where face embeddings are modelled as Gaussian distributions by learning both a mean vector and variance vector. These probabilistic embeddings are learnt by maximising the Mutual Likelihood Score (MLS) between pairs of positive faces [31]. Warburg *et al.* [33] follow a similar approach, introducing a ‘Bayesian Triplet Loss’ to extend training to also include negative probabilistic embeddings. Most recently, STUN [32] was proposed for uncertainty-aware visual place recognition. Cai *et al.* [32] use a student-teacher paradigm to learn a mean vector and variance vector, using the average variance to represent uncertainty. In contrast to our work, they do not explore uncertainty estimation for novel environments, and only explore image-based inputs.

The above approaches estimate aleatoric uncertainty, which arises due to noise or randomness in the input data [10], [31]–[33]. In deep learning, epistemic uncertainty is also present, arising due to the model’s lack of knowledge [10] – this is particularly relevant when testing on data outside the model’s training dataset, such as when traversing to a novel environment in the context of robotics. In contrast to the above works, we use an approach that captures both epistemic and aleatoric uncertainty (through predictive uncertainty estimation).

III. METHODOLOGY

We first define the LPR task, and then introduce uncertainty-aware LPR and our proposed approach.

A. Preliminaries

Given a point cloud P , we require a function that reduces the point cloud to a lower-dimensional vector, referred to as a descriptor \mathbf{d} . As explored in Sec. II-A, state-of-the-art techniques utilise a deeply learnt network parameterised by learnable weights

$$\mathbf{d} = f_{\theta}(P). \quad (1)$$

The network weights are learnt with a training dataset, \mathcal{D} , that contains sets of tuples with an anchor point cloud (P_a), a positive point cloud from the same location (P_{pos}), and a negative point cloud from a different location (P_{neg}). The network weights are trained to maximise the descriptor similarity between all P_a and P_{pos} , and minimise the descriptor similarity between all P_a and P_{neg} – the specific training loss varies depending on the architecture, but often builds off triplet margin loss [34], [35],

$$\mathcal{L}_{triplet} = \max(\|\mathbf{d}_a - \mathbf{d}_{pos}\|_2 - \|\mathbf{d}_a - \mathbf{d}_{neg}\|_2 + \alpha, 0), \quad (2)$$

where α is a minimum margin of difference between the anchor-positive similarity and anchor-negative similarity. In this way, the network learns to produce descriptors that capture the global and local features of a point cloud. Importantly, the features learnt by the network are dictated by the point clouds in the training dataset, *i.e.*, structural features that are omitted from the training dataset may not be learnt by the network.

During evaluation, the LPR task relies on a database \mathbb{D} containing N descriptors with attached location information, $\mathbb{D} = \{\mathbf{d}_1, \dots, \mathbf{d}_N\}$. This database can be a previously curated map or can be collected online as an agent explores an environment. Given a queried location, *i.e.*, a new point cloud from an unknown location P_q , the trained network produces a query descriptor \mathbf{d}_q . This query descriptor is compared to the database descriptors, where the similarity between descriptors is measured via cosine similarity

$$\text{similarity}(\mathbf{d}_q, \mathbf{d}_n) = s_n = \frac{\mathbf{d}_q \cdot \mathbf{d}_n}{\|\mathbf{d}_q\| \|\mathbf{d}_n\|}, \quad n \in \{1, \dots, N\}. \quad (3)$$

A similarity of 1 indicates proportional descriptors and a similarity of -1 indicates opposite descriptors. After calculating all query-database similarities, the database entry

with the greatest similarity is predicted as the matching location to the queried point cloud. If this database location is within a minimum global distance to the true query location, the prediction is considered a correctly predicted revisit, otherwise a false positive, incorrect prediction.

B. Uncertainty-aware Lidar Place Recognition

False-positive revisits arise for queries with no true match in the database, or when a network selects the incorrect database match for a query. In these cases, we need a measure of uncertainty alongside our prediction. Given an uncertainty estimate for the similarity between the query and n -th database entry u_n , and an acceptable uncertainty-rejection threshold (δ), we can reject highly uncertain predictions which may be incorrect,

$$\text{prediction}(u_n, \delta) = \begin{cases} u \leq \delta & n \\ u > \delta & \text{None} \end{cases} \quad (4)$$

For existing networks, a natural measure of uncertainty is the cosine distance between the query and database entry,

$$u_n = 1 - s_n = 1 - \frac{\mathbf{d}_q \cdot \mathbf{d}_n}{\|\mathbf{d}_q\| \|\mathbf{d}_n\|}. \quad (5)$$

As established in the literature [9], [11], [36], deeply learnt networks often have poorly calibrated senses of confidence and uncertainty in their predictions, especially when operating in environments not represented in the training dataset. We propose to use Deep Ensembles [9] of state-of-the-art LPR networks to create the first uncertainty-aware approach to LPR. Deep Ensembles [9] was introduced by Lakshminarayanan *et al.* for uncertainty estimation in simple classification and regression tasks. Below, we describe how we extend it to uncertainty-aware LPR.

We use a homogeneous ensemble of M networks, each parameterised with unique weights

$$\{f_{\theta_1}, f_{\theta_2}, \dots, f_{\theta_M}\}. \quad (6)$$

Each network’s weights are initialised randomly, and the training dataset is randomly shuffled during their training. This is designed to encourage each network to converge to a different set of weights – intuitively, each network finds a different solution (weights) to the same problem (training data).

During evaluation, each member of the ensemble will produce a unique database and query descriptor, and thus we will have a unique set of M similarity scores for all N query-database comparisons

$$\{\{s_{n,m}\}_{m=1}^M\}_{n=1}^N. \quad (7)$$

We approximate each query-database similarity as a Gaussian distribution, with mean and variance as

$$s_{n,\mu} = \frac{1}{M} \sum_{m=1}^M s_{n,m}, \quad (8)$$

$$s_{n,\sigma^2} = \frac{1}{M} \sum_{m=1}^M (s_{n,m} - s_{n,\mu})^2.$$

The database entry with the greatest mean similarity is predicted as the matching location. The mean cosine distance ($1 - s_\mu$) and similarity variance can be used to represent the uncertainty of this prediction. In practice, we find that the mean cosine distance performs best, and thus we use this as our measure of uncertainty.

IV. EVALUATION PROTOCOL

This section proposes a novel evaluation protocol designed to benchmark uncertainty-aware LPR in novel environments and then describes our comparison methods and implementation details.

A. Datasets

We utilise three publicly-available large-scale datasets for our evaluation – the Oxford dataset [1], the NUS Inhouse dataset [1], and the MulRan dataset [37]. We detail the characteristics of each dataset below.

The **Oxford dataset** is a subset of the Oxford RobotCar dataset [38] that was curated by Uy *et al.* [1] for LPR. It contains point cloud submaps from 44 traversals through Oxford, U.K., collected over the course of a year. When evaluating performance on the Oxford dataset, submaps from a single traversal are treated as queries and then evaluated iteratively with submaps from one of the remaining traversals as the database [1]. We follow the standard training and testing dataset split introduced by Uy *et al.* [1].

The **MulRan dataset** [37] consists of traversals of four different environments in South Korea – the Daejeon Convention Center (**DCC**), the **Riverside** of Daejeon city, the Korea Advanced Institute of Science and Technology (KAIST), and Sejong city (Sejong). We use MulRan to test in-session online LPR, where a traversal is evaluated sequentially and the database is collected over the course of the sequence. In this setup, not every query will have a ground-truth database match. We use the DCC and Riverside environments¹, training with DCC traversals 1 and 2 and testing on traversal 3, and training with Riverside traversals 1 and 3 and testing on traversal 2.

The **NUS Inhouse dataset** [1] consists of data from three different regions in Singapore – a university sector (**U.S.**), a residential area (**R.A.**), and a business district (**B.D.**). Point cloud submaps were collected across five traversals of each region at different times. Similar to evaluation on the Oxford dataset, submaps from a single traversal are used as queries and evaluated iteratively with submaps from one of the remaining traversals as the database [1]. We use the standard refined test dataset split [1].

Each dataset represents different urban areas and locations around the world. By training on one environment, and then testing performance on all other dataset environments, we measure the performance of an algorithm on novel

¹In this work, we do not test on the KAIST environment, as it can be considered “solved” with state-of-the-art techniques. Trained on any of the datasets (Oxford, DCC, or Riverside), MinkLoc3D [4] can reliably achieve 97% Recall@1 (or greater) when tested on KAIST. Additionally, we do not test on Sejong city, as it is not configured for in-session LPR.

environments with various levels of similarity to the training environment. Specifically, we use three different training environments – (1) Oxford, (2) DCC, and (3) Riverside, and six different evaluation environments – (1) Oxford, (2) DCC, (3) Riverside, (4) U.S., (5) B.D., and (6) R.A.. This provides a total of 18 possible training-evaluation dataset splits, where 15 test performance in novel environments.

B. Metrics

Uncertainty-aware LPR should be evaluated against two criteria: (1) place recognition capability, *i.e.*, how accurately can a network find a query’s matching entry in a database, and (2) uncertainty estimation, *i.e.*, does the algorithm produce uncertainty estimates that can be used to identify and reject false predictions. We identify three metrics for evaluating against these criteria, as detailed below.

Average Recall@1 is an established metric for quantifying LPR performance [1], [4]–[6], [30]. It calculates the portion of queries that are correctly localised, where the algorithm’s top-1 database match is a ground-truth match with the query. Perfect performance is 100%, and represents all possible revisits being correctly identified.

Area under the Precision Recall curve (AuPR) measures the performance of the estimated uncertainty for rejecting incorrect predictions while retaining correct predictions. It is obtained from the area under the precision-recall curve when rejecting predictions above a specified uncertainty-rejection threshold (δ). Given a set of correct revisit predictions (\mathbb{P}_C) and incorrect predictions (\mathbb{P}_I), the precision and recall for a range of thresholds can be calculated:

$$Precision(\delta) = \frac{|\mathbb{P}_C \leq \delta|}{|\mathbb{P}_C \leq \delta| + |\mathbb{P}_I \leq \delta|} \quad (9)$$

$$Recall(\delta) = \frac{|\mathbb{P}_C \leq \delta|}{|\mathbb{P}_C|} \quad (10)$$

Perfect performance is indicated by an AuPR of 100%, and represents all correct predictions being retained while all incorrect predictions are rejected.

Queries Rejection Rate for 90% Precision jointly quantifies performance for place recognition performance and uncertainty estimation. Given an uncertainty-rejection threshold (δ), where queries with an uncertainty above that threshold are rejected, the remaining predictions will have a precision as defined in Eq. (9). The query rejection rate required to obtain that precision can be defined as:

$$\text{Query Rejection Rate}(\delta) = \frac{|\mathbb{P}_C > \delta| + |\mathbb{P}_I > \delta|}{|\mathbb{P}_C| + |\mathbb{P}_I|} \quad (11)$$

By varying δ , a curve can be constructed of the trade-off between precision and rejection rate [39]. A well-performing system achieves high precision and rejects minimal queries, providing as many accurate revisit predictions as possible. We report the minimum query rejection rate required to achieve a precision of at least 90%. Best performance is a query rejection rate of 0%.

C. Comparison with State-of-the-Art

With no existing approaches for uncertainty-aware LPR, our main comparison is a ‘baseline’ state-of-the-art network using cosine distance as its uncertainty measure. We compare to PointNetVLAD [1], MinkLoc3D [4] and TransLoc3D [6]. We also compare to two techniques for uncertainty-aware image-based retrieval – PFE [31] and STUN [32] – implementing these techniques into MinkLoc3D. For our Deep Ensembles approach, we use $M = 5$ ensemble members. For all single network approaches (baseline, PFE, and STUN), results are calculated from the mean performance of five individually trained networks.

D. Implementation Details

We follow the point cloud pre-processing procedures outlined in [1], [4], [30]. For the Oxford and NUS Inhouse datasets, we follow [1], [4], [6], [30] and define positive and negative training point clouds as within $10m$ and farther than $50m$ of the normalised centroid submaps, respectively. During evaluation, we define a true positive revisit when a prediction is located within $25m$ of a positive ground truth. For the MulRan dataset, we follow [30] and define positive and negative training point clouds within $10m$ and farther than $20m$ of the submap centroid. During evaluation, a query is compared against all point cloud submaps excluding the previous 90s [5], [30], and we define a true positive revisit when a prediction is within $10m$ of the ground truth. Code for all experiments will be made publicly available to enable reproducibility.

V. EXPERIMENTAL RESULTS

We now present the following results: a comparison of the existing baseline with our Deep Ensembles for uncertainty-aware LPR in novel environments, a comparison with image-based uncertainty techniques implemented for LPR, and an ablation on the influence of Deep Ensemble size on performance.

A. Performance in Novel Environments

Table I compares the performance of the baseline networks and our Deep Ensemble networks. Fig. 2 directly quantifies the change in performance when using our Deep Ensembles approach relative to the baseline networks. Across all 18 dataset splits and 3 state-of-the-art architectures, Deep Ensembles consistently improves place recognition (measured by Recall@1) and uncertainty estimation (measured by AuPR), with the most significant improvements observed when testing on novel environments. The effectiveness of our ensembling method is agnostic to the network architecture, with the same trends reflected across MinkLoc3D, TransLoc3D and PointNetVLAD.

As expected, all networks show best performance when trained and evaluated in the same environment. In this scenario, on average, Deep Ensembles improves Recall@1 by 1.6%, 4%, and 3% and AuPR by 0.6%, 2.2%, and 1.1% for MinkLoc3D, TransLoc3D and PointNetVLAD, respectively. While this performance improvement is desirable, Deep

TABLE I: Across all architectures and all dataset combinations, our Deep Ensembles approach consistently exhibits superior place recognition (measured by Recall@1) and uncertainty estimation (measured by AuPR). Best performance is indicated in bold.

Trained on:			Tested on:											
			Oxford		DCC		Riverside		B.D.		R.A.		U.S.	
			R@1	AuPR	R@1	AuPR	R@1	AuPR	R@1	AuPR	R@1	AuPR	R@1	AuPR
Oxford	MinkLoc3D	Baseline	92.8	99.3	61.1	83.8	61.4	82.2	78.7	96.4	79.4	94.8	83.7	96.3
		Ensemble	95.5	99.7	67.4	87.9	63.8	88.1	84.5	97.9	87.2	97.4	89.4	97.9
	TransLoc3D	Baseline	91.1	98.6	48.2	45.4	46.0	32.9	74.6	89.2	71.8	90.0	79.1	92.7
		Ensemble	94.8	99.4	53.7	50.7	49.3	36.6	83.5	96.0	84.2	96.1	89.0	97.5
	PointNetVLAD	Baseline	77.9	93.1	36.1	85.6	59.2	83.9	66.5	93.6	68.1	93.6	71.6	94.2
		Ensemble	81.1	94.0	37.9	87.6	60.5	85.8	70.4	95.1	72.1	94.9	76.9	95.5
DCC	MinkLoc3D	Baseline	65.7	91.1	87.2	97.3	65.8	88.5	73.3	95.1	75.0	93.1	81.6	97.1
		Ensemble	71.2	94.2	89.1	98.0	66.6	91.3	79.3	96.9	80.2	95.4	86.1	98.3
	TransLoc3D	Baseline	60.2	72.2	75.4	87.2	52.8	40.1	69.1	86.0	67.9	86.8	79.6	92.1
		Ensemble	69.0	81.1	78.8	89.2	54.5	42.2	78.7	93.0	78.9	94.8	87.2	95.2
	PointNetVLAD	Baseline	45.0	77.5	63.8	86.1	61.1	65.8	56.7	88.4	54.6	86.4	58.6	88.0
		Ensemble	54.6	85.3	69.1	87.7	62.6	68.6	64.1	92.1	65.1	91.7	66.5	92.1
Riverside	MinkLoc3D	Baseline	68.5	91.5	51.5	95.3	76.9	95.0	78.7	96.7	81.1	94.7	86.1	98.1
		Ensemble	73.3	94.2	52.3	95.6	77.1	95.8	82.9	97.7	85.6	96.4	89.1	98.8
	TransLoc3D	Baseline	60.6	79.7	48.6	83.2	78.0	81.1	75.9	93.0	74.5	91.7	83.6	94.9
		Ensemble	69.4	87.8	51.5	85.8	83.0	84.9	83.5	96.6	83.3	96.4	90.8	97.3
	PointNetVLAD	Baseline	47.7	82.9	45.5	93.8	65.4	90.2	59.0	90.4	59.4	88.5	63.2	91.7
		Ensemble	51.4	85.5	45.9	94.7	66.1	91.1	62.7	92.0	63.6	90.9	66.3	93.1

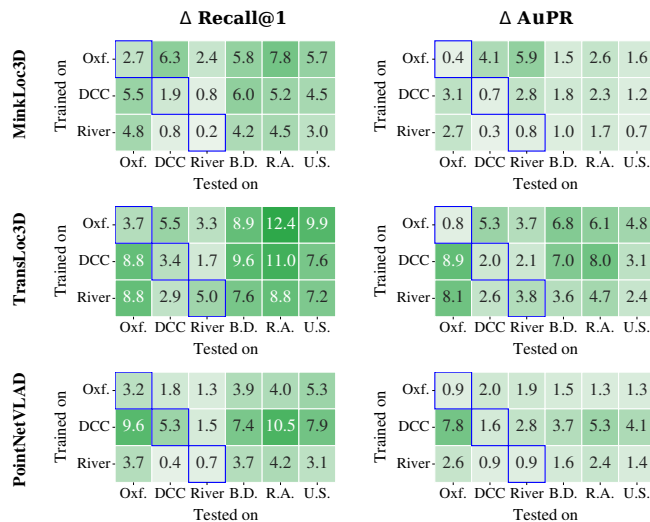


Fig. 2: Illustration of the performance increase gained by Deep Ensembles relative to a baseline network. Results where the training and testing environment are consistent are outlined in blue.

Ensembles show a significantly greater improvement when networks are evaluated on novel environments – on average, Deep Ensembles improves Recall@1 by 4.5%, 7.6%, and 4.6% and AuPR by 2.2%, 5.2%, and 2.7% for MinkLoc3D, TransLoc3D and PointNetVLAD, respectively.

For each dataset split and architecture, Fig. 3 visualises the minimum query rejection rate required to obtain 90% precision in the remaining queries. Deep Ensembles consistently obtains 90% precision with fewer rejections compared to the baseline, effectively using uncertainty to reject incorrect predictions. Again, the improvement is most significant when networks test on novel environments – approximately a 5 – 15% decrease for PointNetVLAD, 10 – 20% for MinkLoc3D, and up to 40% decrease in rejection rates for TransLoc3D. This improvement becomes smaller when

tested on environments that are highly similar to the training dataset – for example, when training on DCC and testing on Riverside (or vice-versa), as these are both collected from urban roads in Daejeon, South Korea. In some cases, both the baseline networks and Deep Ensembles achieve 90% precision without needing to reject any queries, or are unable to achieve 90% precision even when rejecting all queries – here, the performance of the baseline and Deep Ensembles are equal. Finally, while TransLoc3D sees the greatest relative improvement when using uncertainty-aware Deep Ensembles, MinkLoc3D shows the overall best performance for performing uncertainty-aware LPR.

B. Comparison with Image-based Uncertainty Methods

We compare to state-of-the-art approaches for uncertainty-aware image-based retrieval in Table II. Overall, we find that PFE [31] and STUN [32] are unable to reliably estimate uncertainty for LPR (as measured by AuPR), nearly always performing worse than the baseline network. While both techniques have shown impressive performance in the image domain, this highlights a potential discrepancy between the challenges of uncertainty estimation for image versus point cloud modalities. Additionally, we note that both techniques are able to maintain general place recognition performance – the Recall@1 is 94.4%, 94.4%, and 94.3% on average for the baseline, PFE, and STUN, respectively.

Given an average baseline AuPR of 93.7% across 18 dataset splits, PFE and STUN produce an average performance decline in uncertainty estimation of -1.2% and -26.1% respectively, while our approach shows a mean improvement of 2.0% . Both PFE and STUN follow a similar approach – learning a ‘variance’ for each descriptor during training, and using this to approximate aleatoric uncertainty during evaluation. This differs to Deep Ensembles, which produces predictive uncertainty estimates that capture both aleatoric and epistemic uncertainty. When computing its uncertainty, PFE considers both the predicted variance of the

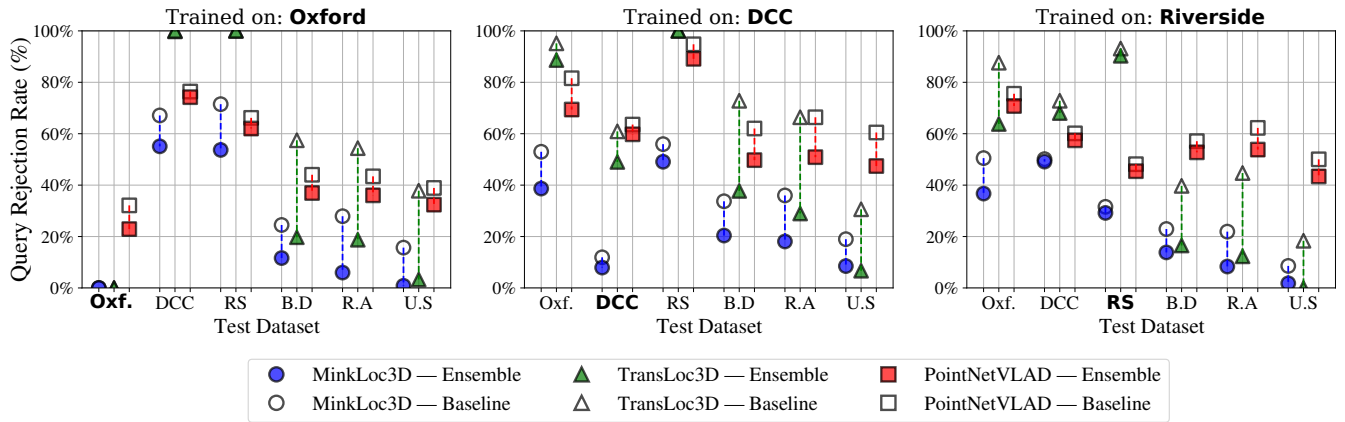


Fig. 3: How many uncertain queries must be rejected to ensure that all remaining queries have a 90% precision? Our Deep Ensembles approach consistently enables rejection of fewer queries.

TABLE II: Our Deep Ensembles approach, based on MinkLoc3D, achieves best performance for uncertainty estimation when compared against state-of-the-art techniques for uncertainty-aware image retrieval tasks. Performance is indicated relative to the baseline model (Δ AuPR), and best performance is highlighted in bold.

	Tested:	Baseline	PFE [31]	STUN [32]	DEns. (Ours)
		AuPR	Δ AuPR	Δ AuPR	Δ AuPR
Trained on Oxford	Oxf.	99.3	-0.1	-7.0	0.4
	DCC	83.8	-9.3	-44.2	4.1
	RS	82.2	-9.9	-47.8	5.9
	B.D.	96.4	-0.2	-15.0	1.5
	R.A.	94.8	0.3	-15.7	2.7
	U.S.	96.3	0.0	-14.7	1.6
Trained on DCC	Oxf.	91.1	-1.5	-19.0	3.2
	DCC	97.3	0.0	-34.6	0.7
	RS	88.5	2.8	-44.9	2.8
	B.D.	95.1	-0.7	-22.3	1.8
	R.A.	93.1	-1.3	-19.1	2.4
	U.S.	97.1	-0.2	-19.9	1.1
Trained on Riverside	Oxf.	91.5	-0.8	-18.1	2.8
	DCC	95.3	0.0	-54.3	0.4
	RS	95.0	-0.5	-49.8	0.8
	B.D.	96.7	-0.3	-17.5	1.0
	R.A.	94.7	-0.2	-14.5	1.7
	U.S.	98.1	0.0	-12.0	0.7
Average Results		93.7	-1.2	-26.1	2.0

query and the top-1 database descriptor. In contrast, STUN uses only the variance predicted for the query descriptor, potentially contributing to its lower performance. Overall, it can be inferred that aleatoric uncertainty estimation may not be sufficient for uncertainty-aware LPR, particularly when operating in novel environments, where epistemic uncertainty is more relevant [10], [11].

C. Ensemble Ablation

In Fig. 4, we visualise the effect of Deep Ensemble size on the Recall@1 and AuPR relative to the baseline MinkLoc3D. As more models are added into the ensemble, the Recall@1 and AuPR of the Deep Ensemble increases. This highlights the performance-computation trade-off inherent to any ensembling approach. Testing on a NVIDIA GeForce RTX 2080, we were able to run five MinkLoc3D models in parallel with a batch size of 8, effectively implementing a

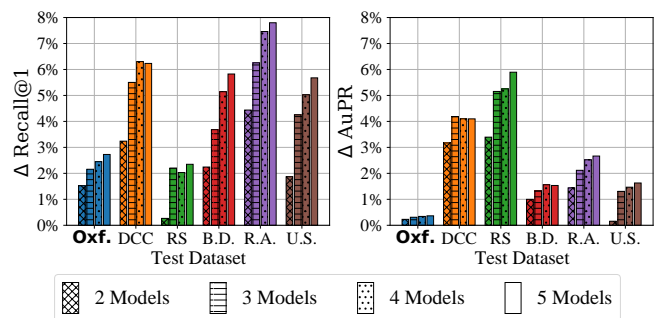


Fig. 4: For MinkLoc3D trained on Oxford, we visualise how the size of the ensemble influences the increase in performance when compared to the baseline MinkLoc3D.

5-model Deep Ensemble that can run 90 tests/second. We note that the performance change with increasing models is not linear, and a Deep Ensemble with at least three models can consistently achieve results within 2% of the 5-model Deep Ensemble.

VI. CONCLUSION

In this paper, we have investigated uncertainty-aware lidar place recognition (LPR), where networks must produce an uncertainty estimate that can be used to identify and reject false revisit predictions. We proposed a novel evaluation protocol for benchmarking uncertainty-aware LPR that particularly focuses on performance in novel environments, and introduced the first uncertainty-aware LPR network with a Deep Ensembles approach. We show Deep Ensembles consistently improves place recognition performance and uncertainty evaluation for state-of-the-art architectures MinkLoc3D, PointNetVLAD and TransLoc3D. Deep Ensembles also consistently outperforms state-of-the-art image retrieval techniques that estimate only aleatoric uncertainty, motivating further research specifically targeting uncertainty-aware LPR. Future work could also explore how uncertainty-aware LPR can be used to infer uncertainty in robot pose estimation for loop-closure detection.

REFERENCES

- [1] M. A. Uy and G. H. Lee, "PointNetVLAD: Deep Point Cloud Based Retrieval for Large-Scale Place Recognition," in *Proceedings of the IEEE Conference on Computer Vision and Pattern Recognition*, June 2018, pp. 4470–4479.
- [2] W. Zhang and C. Xiao, "PCAN: 3D Attention Map Learning Using Contextual Information for Point Cloud Based Retrieval," in *Proceedings of the IEEE/CVF Conference on Computer Vision and Pattern Recognition*, June 2019.
- [3] Z. Liu, S. Zhou, C. Suo, P. Yin, W. Chen, H. Wang, H. Li, and Y.-H. Liu, "LPD-Net: 3D Point Cloud Learning for Large-Scale Place Recognition and Environment Analysis," in *Proceedings of the IEEE/CVF International Conference on Computer Vision*, October 2019.
- [4] J. Komorowski, "MinkLoc3D: Point Cloud Based Large-Scale Place Recognition," in *Proceedings of the IEEE/CVF Winter Conference on Applications of Computer Vision*, 2021, pp. 1790–1799.
- [5] K. Vidanapathirana, M. Ramezani, P. Moghadam, S. Sridharan, and C. Fookes, "LoGG3D-Net: Locally Guided Global Descriptor Learning for 3D Place Recognition," *Proceedings of the IEEE International Conference on Robotics and Automation*, 2022.
- [6] T.-X. Xu, Y.-C. Guo, Y.-K. Lai, and S.-H. Zhang, "TransLoc3D : Point Cloud based Large-scale Place Recognition using Adaptive Receptive Fields," in *Proceedings of the International Conference on Computational Visual Media*, 2022.
- [7] D. Amodei, C. Olah, J. Steinhardt, P. Christiano, J. Schulman, and D. Mané, "Concrete problems in AI safety," *arXiv preprint arXiv:1606.06565*, 2016.
- [8] N. Sünderhauf, O. Brock, W. Scheirer, R. Hadsell, D. Fox, J. Leitner, B. Upcroft, P. Abbeel, W. Burgard, M. Milford *et al.*, "The limits and potentials of deep learning for robotics," *The International journal of robotics research*, vol. 37, no. 4-5, pp. 405–420, 2018.
- [9] B. Lakshminarayanan, A. Pritzel, and C. Blundell, "Simple and Scalable Predictive Uncertainty Estimation using Deep Ensembles," *Advances in neural information processing systems*, vol. 30, 2017.
- [10] A. Kendall and Y. Gal, "What Uncertainties Do We Need in Bayesian Deep Learning for Computer Vision?" *Advances in neural information processing systems*, vol. 30, 2017.
- [11] D. Miller, L. Nicholson, F. Dayoub, and N. Sünderhauf, "Dropout Sampling for Robust Object Detection in Open-Set Conditions," in *Proceedings of the IEEE International Conference on Robotics and Automation*. IEEE, 2018, pp. 3243–3249.
- [12] D. Miller, N. Sünderhauf, M. Milford, and F. Dayoub, "Uncertainty for Identifying Open-Set Errors in Visual Object Detection," *IEEE Robotics and Automation Letters*, vol. 7, no. 1, pp. 215–222, 2021.
- [13] S. Salti, F. Tombari, and L. Di Stefano, "SHOT: Unique signatures of histograms for surface and texture description," *Computer Vision and Image Understanding*, vol. 125, pp. 251–264, 2014.
- [14] M. Bosse and R. Zlot, "Place recognition using keypoint voting in large 3D lidar datasets," in *Proceedings of the IEEE International Conference on Robotics and Automation*, 2013, pp. 2677–2684.
- [15] R. B. Rusu, N. Blodow, and M. Beetz, "Fast Point Feature Histograms (FPFH) for 3D registration," in *Proceedings of the IEEE International Conference on Robotics and Automation*, 2009, pp. 3212–3217.
- [16] G. Kim and A. Kim, "Scan Context: Egocentric Spatial Descriptor for Place Recognition Within 3D Point Cloud Map," in *Proceedings of the IEEE/RSJ International Conference on Intelligent Robots and Systems*, 2018, pp. 4802–4809.
- [17] G. Kim, S. Choi, and A. Kim, "Scan Context++: Structural Place Recognition Robust to Rotation and Lateral Variations in Urban Environments," *IEEE Transactions on Robotics*, 2021.
- [18] C. Qi, H. Su, K. Mo, and L. J. Guibas, "PointNet: Deep Learning on Point Sets for 3D Classification and Segmentation," *Proceedings of the IEEE/CVF Conference on Computer Vision and Pattern Recognition*, pp. 77–85, 2017.
- [19] L. Hui, H. Yang, M. Cheng, J. Xie, and J. Yang, "Pyramid point cloud transformer for large-scale place recognition," *Proceedings of the IEEE/CVF International Conference on Computer Vision*, pp. 6078–6087, 2021.
- [20] J. Komorowski, "Improving Point Cloud Based Place Recognition with Ranking-based Loss and Large Batch Training," *Proceedings of the International Conference on Pattern Recognition*, 2022.
- [21] R. Arandjelović, P. Gronát, A. Torii, T. Pajdla, and J. Sivic, "NetVLAD: CNN Architecture for Weakly Supervised Place Recognition," *IEEE Transactions on Pattern Analysis and Machine Intelligence*, vol. 40, pp. 1437–1451, 2018.
- [22] F. Radenović, G. Toliás, and O. Chum, "Fine-tuning CNN Image Retrieval with No Human Annotation," *IEEE Transactions on Pattern Analysis and Machine Intelligence*, vol. PP, 11 2017.
- [23] K. Vidanapathirana, P. Moghadam, B. Harwood, M. Zhao, S. Sridharan, and C. Fookes, "Locus: LiDAR-based Place Recognition using Spatiotemporal Higher-Order Pooling," *Proceedings of the IEEE International Conference on Robotics and Automation*, pp. 5075–5081, 2021.
- [24] D. Feng, L. Rosenbaum, F. Timm, and K. Dietmayer, "Leveraging Heteroscedastic Aleatoric Uncertainties for Robust Real-Time LiDAR 3D Object Detection," in *IEEE Intelligent Vehicles Symposium*. IEEE, 2019, pp. 1280–1287.
- [25] D. Feng, L. Rosenbaum, and K. Dietmayer, "Towards Safe Autonomous Driving: Capture Uncertainty in the Deep Neural Network For Lidar 3D Vehicle Detection," in *Proceedings of the IEEE International Conference on Intelligent Transportation Systems*. IEEE, 2018, pp. 3266–3273.
- [26] H. Pan, Z. Wang, W. Zhan, and M. Tomizuka, "Towards Better Performance and More Explainable Uncertainty for 3D Object Detection of Autonomous Vehicles," in *Proceedings of the IEEE International Conference on Intelligent Transportation Systems*. IEEE, 2020, pp. 1–7.
- [27] S. Wirges, M. Reith-Braun, M. Lauer, and C. Stiller, "Capturing object detection uncertainty in multi-layer grid maps," in *IEEE Intelligent Vehicles Symposium*. IEEE, 2019, pp. 1520–1526.
- [28] G. P. Meyer and N. Thakurdesai, "Learning an uncertainty-aware object detector for autonomous driving," in *Proceedings of the IEEE/RSJ International Conference on Intelligent Robots and Systems*. IEEE, 2020, pp. 10 521–10 527.
- [29] T. Cortinhal, G. Tzelepis, and E. Erdal Aksoy, "SalsaNext: Fast, Uncertainty-Aware Semantic Segmentation of LiDAR Point Clouds," in *International Symposium on Visual Computing*. Springer, 2020, pp. 207–222.
- [30] J. Knights, P. Moghadam, M. Ramezani, S. Sridharan, and C. Fookes, "InCloud: Incremental Learning for Point Cloud Place Recognition," in *Proceedings of the IEEE/RSJ International Conference on Intelligent Robots and Systems*, 2022.
- [31] Y. Shi and A. K. Jain, "Probabilistic Face Embeddings," in *Proceedings of the IEEE/CVF International Conference on Computer Vision*, 2019, pp. 6902–6911.
- [32] K. Cai, C. X. Lu, and X. Huang, "STUN: Self-Teaching Uncertainty Estimation for Place Recognition," *arXiv preprint arXiv:2203.01851*, 2022.
- [33] F. Warburg, M. Jørgensen, J. Civera, and S. Hauberg, "Bayesian Triplet Loss: Uncertainty Quantification in Image Retrieval," in *Proceedings of the IEEE/CVF International Conference on Computer Vision*, 2021, pp. 12 158–12 168.
- [34] A. Hermans, L. Beyer, and B. Leibe, "In defense of the triplet loss for person re-identification," *arXiv preprint arXiv:1703.07737*, 2017.
- [35] F. Schroff, D. Kalenichenko, and J. Philbin, "FaceNet: A Unified Embedding for Face Recognition and Clustering," in *Proceedings of the IEEE Conference on Computer Vision and Pattern Recognition*, June 2015.
- [36] C. Guo, G. Pleiss, Y. Sun, and K. Q. Weinberger, "On Calibration of Modern Neural Networks," in *Proceedings of the International Conference on Machine Learning*. PMLR, 2017, pp. 1321–1330.
- [37] G. Kim, Y. S. Park, Y. Cho, J. Jeong, and A. Kim, "MulRan: Multimodal Range Dataset for Urban Place Recognition," in *Proceedings of the IEEE International Conference on Robotics and Automation*. IEEE, 2020, pp. 6246–6253.
- [38] W. Maddern, G. Pascoe, C. Linegar, and P. Newman, "1 Year, 1000km: The Oxford RobotCar Dataset," *The International Journal of Robotics Research*, vol. 36, no. 1, pp. 3–15, 2017.
- [39] P. Grother and E. Tabassi, "Performance of Biometric Quality Measures," *IEEE Transactions on Pattern Analysis and Machine Intelligence*, vol. 29, no. 4, pp. 531–543, 2007.